Simulating the dPFG and qMAS in a Model of Acute Axonal Injury

Matthew Budde[1] and Nathan Skinner[2]

[1]Neurosurgery, Medical College of Wisconsin, Milwaukee, Wisconsin, United States, [2]Biophysics, Medical College of Wisconsin, Milwaukee, Wisconsin, United States

TARGET AUDIENCE: Investigators and clinicians looking to improve detection of disease and injury in the central nervous system.

PURPOSE: Fractional anisotropy (FA) derived from diffusion tensor imaging (DTI) is a sensitive marker of injury in the brain and spinal cord, but it is limited by assumptions of coherent macroscopic organization. Diffusion measured parallel to axonal fibers has been shown to be a marker of axonal injury, but the presence of crossing fibers confounds this relationship. Two novel diffusion weighted imaging techniques, the double pulse field gradient[1] (dPFG) and q-vector magic angle spinning[2] (qMAS), reportedly detect the microscopic anisotropy without complication from the macroscopic anisotropy. Here, we performed a computational simulation of the dPFG and qMAS sequences in a model of acute axonal injury and compared the derived measures to DTI and diffusion kurtosis imaging (DKI) measures of injury.

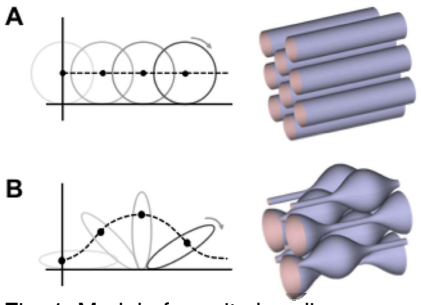

Fig. 1. Model of neurite beading.

METHODS: Beaded axons (Fig. 1), were modeled as previously described[3], and consisted of uniform diameters from 1 to 8 um and intracellular volume fractions from 0.4 to 0.78. Fiber dispersion and crossing fibers were also modeled. Monte-carlo random walk simulations were performed with Camino[4], and consisted of 50,000 spins, 2000 time steps, free diffusivity of 1.8 mm^2/ms, and impermeable surfaces. The DWI sequences (Fig. 2) consisted of a pulsed gradient spin echo (PGSE) (30 directions; gradient duration (δ) of 3 ms; separation (Δ) of 48 ms), the double-pulsed field gradient[1] (dPFG) (60 parallel and 60 orthogonal directions; δ of 3 ms, Δ of 12.5, and mixing time (τ) of 5 ms), and the q-vector magic angle spinning (qMAS) with modulated gradients[2] (30 separate directions; separation time (Δ_{mas}) of 45 ms). Ten b-values were simulated for each sequence up to a maximum of 7500 s/mm^2. T_2 effects were ignored, and no additional noise was added. Measures of microscopic anisotropy were derived for the dPFG and qMAS as fractional eccentricity (FE) and microscopic FA (μFA), respectively, and compared with FA and mean kurtosis (MK) derived from DTI and DKI, respectively.

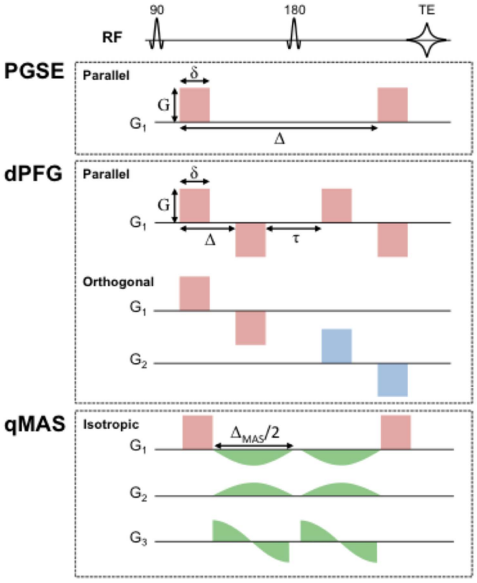

Fig. 2 DWI pulse sequences.

RESULTS: The results confirm the expected isotropic diffusion weighting behavior of the qMAS (not shown), as rotation of the qMAS encoding did not change with orientation. Second, the results reinforce that FA as a marker of acute injury is confounded by fiber dispersion and crossing (Fig. 3). In contrast, DKI, dPFG, and qMAS all eliminate the effects of macroscopic anisotropy (Fig. 3). The dPFG and qMAS sequences have greater sensitivity (% change) for beaded axons compared to the unbeaded form. However, each of these measures were also affected by the volume fraction(not shown), indicating edema could potentially complicate their interpretation.

DISCUSSION: The simulated results for the novel diffusion weighted imaging sequences demonstrate a greater sensitivity to beaded neurites. Beading is believed to be an important biophysical mechanism in acute axonal injury due to cerebral ischemia, spinal cord injury, traumatic brain injury, and other acute neurological disorders. The results demonstrate that the dPFG and qMAS sequences will likely have important diagnostic utility as markers of injury, although experimental validation and histological verification are necessary for a better understanding of their specificity for injury and how they relate to other features such as edema and inflammation.

CONCLUSION: The simulations demonstrate that both the dPFG and qMAS DWI sequences are both sensitive to the effects of axonal beading without complication from the macroscopic fiber organization and therefore have significant investigative and clinical implications for better understanding CNS pathology and future imaging applications.

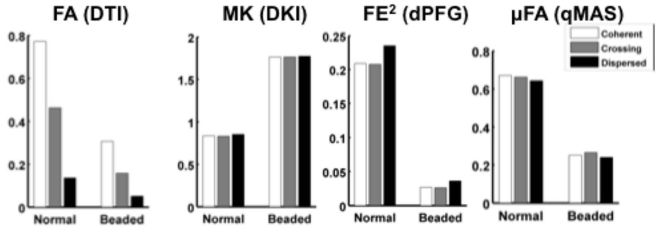

Fig. 3. Simulated parameters in various fiber configurations and effect of beading.

REFERENCES: **1**. Jespersen S, et al. NMR Biomed. 2013; **2**. Lasič S, et al. FrontPhys. 2014; **3.** Budde, et al. PNAS 2010;